

Variations in normal color vision.

I. Cone-opponent axes

Michael A. Webster

Department of Psychology, University of Nevada, Reno, Reno, Nevada 89557

Eriko Miyahara

Department of Psychology, Rochester Institute of Technology, Rochester, New York 14623

Gokhan Malkoc and Vincent E. Raker

Department of Psychology, University of Nevada, Reno, Reno, Nevada 89557

Received October 14, 1999; revised manuscript received May 17, 2000; accepted May 25, 2000

Early postreceptoral color vision is thought to be organized in terms of two principal axes corresponding to opposing L- and M-cone signals (LvsM) or to S-cone signals opposed by a combination of L- and M-cone signals (SvsLM). These cone-opponent axes are now widely used in studies of color vision, but in most cases the corresponding stimulus variations are defined only theoretically, based on a standard observer. We examined the range and implications of interobserver variations in the cone-opponent axes. We used chromatic adaptation to empirically define the LvsM and SvsLM axes and used both thresholds and color contrast adaptation to determine sensitivity to the axes. We also examined the axis variations implied by individual differences in the color matching data of Stiles and Burch [Opt. Acta **6**, 1 (1959)]. The axes estimated for individuals can differ measurably from the nominal standard-observer axes and can influence the interpretation of postreceptoral color organization (e.g., regarding interactions between the two axes). Thus, like luminance sensitivity, individual differences in chromatic sensitivity may be important to consider in studies of the cone-opponent axes. © 2000 Optical Society of America [S0740-3232(00)01209-6]

OCIS codes: 330.1690, 330.1720, 330.1730, 330.5020, 330.7310.

1. INTRODUCTION

A central goal in the study of color vision is to understand how color information is represented at different stages of the visual system. At the level of the receptors, this representation is in terms of the excitations in the long-, medium-, or short-wavelength-sensitive (L, M, or S) cones, while at postreceptoral levels it corresponds instead to different combinations of the cone signals. Electrophysiological recordings from the retina and lateral geniculate^{1,2} and psychophysical measurements of chromatic sensitivity³⁻⁸ suggest that the cone signals are organized along two dimensions that correspond to opposing signals from the L and M cones (LvsM) or to signals from the S cones opposed by a combination of signals from the L and M cones (SvsLM). Differences in the genes encoding the cone pigments suggest that these two chromatic dimensions represent two subsystems of color vision that evolved at different times.⁹ The LvsM and SvsLM axes differ from the principal axes implied by color appearance, and some measures of sensitivity point both to interactions between the two axes^{10,11} and to further mechanisms tuned to intermediate color directions.¹² Yet along with luminance, the LvsM and SvsLM axes are thought to define the cardinal axes underlying early postreceptoral color coding.

Stimuli defined by the cardinal axes are now widely used in vision research. It is well recognized that for

chromatic variations to be isolated, the luminances of different colors must be equated empirically for individual observers, for there are large individual differences in luminance sensitivity.¹³ Many psychophysical procedures have been developed to assess luminance sensitivity.¹⁴ However, with rare exceptions the SvsLM and LvsM dimensions within the chromatic plane are defined only theoretically, on the basis of a standard observer. Measurements of the variability in these chromatic dimensions are therefore important for assessing whether a nominal stimulus specification is adequate for defining the cardinal axes. We examined variability in the LvsM and SvsLM axes both empirically and theoretically and show that variations from the nominal axes can be large enough to influence color measurements and their interpretation. In the accompanying paper we explore how variations in these axes are related to variations in phenomenal color appearance.¹⁵

2. METHODS

Stimuli were presented on a Nano T2.20 monitor controlled by a Cambridge Research Systems VSG graphics card. The framebuffer allowed luminances to be specified with a resolution of 12 bits per gun. Gun luminances and spectra were calibrated with a Photo Research PR650

spectroradiometer, and luminances were linearized through lookup tables. CIE 1931 x, y chromaticities of the phosphors were measured to be 0.618, 0.344 (red), 0.281, 0.605 (green), and 0.150, 0.063 (blue).

The stimuli had a mean luminance of 30 cd/m^2 and varied around a mean chromaticity equivalent to Illuminant C (CIE 1931 $x, y = 0.31, 0.316$). Stimulus chromaticities were defined relative to this zero-contrast background by their angle (\sim hue) and contrast (\sim saturation) within a scaled version of the MacLeod–Boynton¹⁶ chromaticity diagram. Within this opponent-modulation space¹⁷ a hue angle of 0 deg corresponded to increasing L-cone excitation along the LvsM axis, and an angle of 90 deg corresponded to increasing S-cone excitation along the SvsLM axis. This space was used to measure and represent individual observers' results within a common space defined by a standard observer. The angles and sensitivities defining the chromatic axes for individual observers within this space were determined empirically as part of the focus of the present study. For the principal observers, luminances were defined for individuals based on minimum-motion settings.¹⁸ The relationship between our LvsM and SvsLM coordinates and r, b coordinates of the MacLeod–Boynton space is given by

$$\text{LvsM contrast} = (r_{\text{mb}} - 0.6568) * 2754$$

$$\text{SvsLM contrast} = (b_{\text{mb}} - 0.01825) * 4099$$

where 0.6568, 0.01825 are the MacLeod–Boynton coordinates of Illuminant C and 2754, 4099 are the constants that scale contrasts along the LvsM and SvsLM axes, respectively. These constants were chosen so that a unit distance along each axis corresponded to the threshold for detecting the color change away from white along either axis and were based on initial estimates of the average thresholds for four observers. Further measurements based on five observers collected during the actual study were closely consistent with these averages. Compared with the scaling constants that we have adopted previously to equate the strength of contrast adaptation effects along the cardinal axes,^{19,20} the present factors represent an increase of 1.4 times in the presumed sensitivity to the LvsM axis and a sensitivity decrease of 1.35 times in the SvsLM axis. These differences may reflect differences in the relative weighting of the two axes in threshold detection and suprathreshold adaptation tasks (see below).

We used a variety of tasks to assess sensitivity to the test stimuli. Conditions specific to each task are described in the relevant parts of Section 3. In all cases colors were presented as uniform square patches within 2-deg fields, delimited from the background by narrow black borders. The surrounding background subtended 6.4×8.4 deg and was maintained at the background color (i.e., 30 cd/m^2 and zero chromatic contrast). The room was otherwise dark. Observers viewed the display monocularly from a distance of 250 cm and fixated the center of the field or, when two fields were present, a small black fixation cross midway between the fields. Each run began with a 3-min period of adaptation, either to steady backgrounds that remained present throughout the run or to temporal (1-Hz) modulations of color in the field, that were interleaved with each test presentation.

On each trial, test stimuli were shown within the field at full contrast for 280 ms and were ramped on and off with Gaussian envelopes ($\sigma = 80$ ms). The observers included the authors and two additional subjects. All subjects had normal color vision as assessed by the Ishihara pseudoisochromatic plates.

3. RESULTS

A. LvsM and SvsLM Cone-Opponent Axes

1. Cone-Opponent Axes Estimated from Threshold Contours

We characterized variations in the cone-opponent axes across observers by examining differences both in the chromatic angles defining the LvsM and SvsLM axes and in the relative sensitivity to the two axes. The angles corresponding to the SvsLM and LvsM axes were estimated by using variants of a chromatic adaptation method described by Webster *et al.*²¹ and Webster and Mollon.⁸ In this task, thresholds for detecting a color change along different directions in color space are measured in the presence of an adapting background chosen to selectively desensitize different classes of cones. The background field was formed by illuminating a diffusing screen with light from a slide projector and was combined with the monitor by viewing both the display and the background through a beam splitter. Light from the projector passed through color filters that were chosen to transmit either short (Wratten 47B) or long (Wratten 25) wavelengths. The luminance of the background was adjusted for different filters and observers by the addition of neutral density filters so that thresholds were measurable for all chromatic angles but changed by at least 1 log unit for the most affected color directions.

The Wratten 25 filter transmits only long (>580 nm) wavelengths and thus strongly desensitizes L and M cones while negligibly affecting S cones. Thresholds in the presence of this background should therefore be elevated most for stimuli that cannot be detected by the S cones or, in other words, for stimuli that vary along an axis of constant S-cone excitation (the LvsM axis). Alternatively, the Wratten 47B filter passes only shorter visible wavelengths (<500 nm) and thus most strongly light adapts the S cones. Thus in this case the largest threshold changes should occur for stimuli that depend on detection only by S cones or, in other words, for the constant-LM (SvsLM) axis. Webster *et al.*²¹ and Webster and Mollon⁸ used this technique to determine the LvsM and SvsLM axes by measuring thresholds for a range of chromatic angles bracketing either nominal cardinal axis. In the present case we instead measured complete threshold contours by probing detection along different directions within the LvsM and SvsLM plane. The thresholds were estimated with use of a spatial forced-choice task in which the test pulse was presented in a 2-deg field above or below fixation, with the test contrast varied over trials according to the QUEST procedure.²² Observers made six to eight settings at each chromatic angle. Ellipses were then fitted to the mean thresholds to estimate the angle of maximum sensitivity loss.

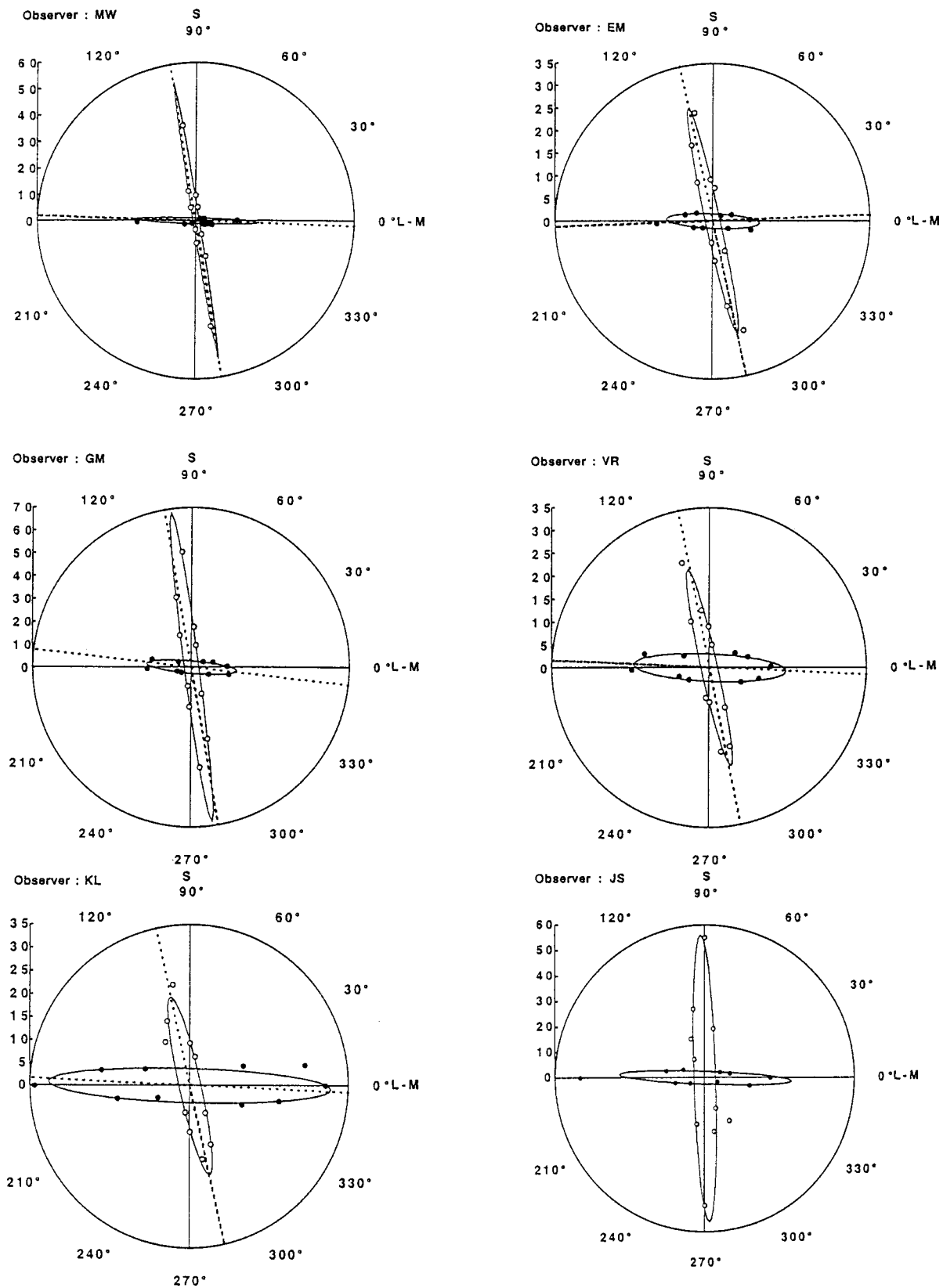


Fig. 1. Estimates of the cone-opponent axes based on chromatic adaptation. Points and fitted ellipses plot the thresholds for detecting chromatic pulses in the presence of a short- or long-wavelength adapting background. Short-wavelength backgrounds selectively elevate thresholds along the SvsLM axis, and long-wavelength backgrounds elevate thresholds along the LvsM axis. Axes were estimated from the orientation of the threshold ellipses or from contrast matching in the presence of the backgrounds (dashed lines through ellipses; see text). Each panel plots the results for a different observer. Axes for JS were estimated only by the threshold task.

Figure 1 shows the threshold contours for both adapting backgrounds. Each panel plots the results for a different observer. The contours are largely symmetrical about the origin and are well described by ellipses. Moreover, the threshold changes along each axis are highly selective, suggesting that they can accurately define the chromatic axes by the direction of maximum sensitivity loss. (In the present study we defined this direction by the orientation of the ellipse fitted to the thresholds in the presence of the adapting field. However, essentially the same estimates are given by taking instead the maximum *change* in thresholds between the chromatic and the neutral adaptation conditions.^{8,21}) The estimates for the LvsM axis for six observers have a mean of -2.6 deg and ranged from -4.8 to -1.6 deg. They therefore differ slightly from the nominal LvsM angle of 0 deg. On the other hand, the contours on the short-wavelength background are more conspicuously tilted relative to the nominal SvsLM axis at 90 deg (mean angle= 99.6 deg and range from 91.8 to 102.7 deg). These deviations are similar to those found previously by Webster *et al.*²¹ and Webster and Mollon⁸ for different observers and displays.

2. Cone-Opponent Axes Estimated from Contrast Matching

The measurement of threshold contours provides a precise specification of the sensitivity losses but is time consuming. As a more rapid method of defining the angle of maximum sensitivity loss, we developed an alternative procedure based on contrast matching. The method is similar in logic to a paradigm developed by Webster and Mollon²³ to estimate the equiluminance point in heterochromatic flicker photometry and is illustrated in Fig. 2. In this case the stimulus consisted of a pair of colors, presented simultaneously in fields above and below fixation. The two colors had the same contrast (i.e., distance from the origin within our color space, typically 30 – 40) but differed in color direction. The chromatic angle between the two stimuli was fixed at 10 deg, while the mean angle of the pair was varied across trials. On each trial the colors were randomly assigned to the top and bottom field, and observers judged which field appeared to have the higher contrast. (The method thus requires that contrasts be compared across stimuli that differ in hue, yet such judgments can be made reliably²⁴ and were facilitated in our task by keeping contrasts and hue differences at moderately low values.)

Figure 2 shows the results expected in the presence of the short-wavelength background, which, again, strongly elongates threshold contours along the SvsLM axis. Because of this, hue angles that are closer to the S axis will be closer to threshold and thus should appear lower in contrast. For the color pair in the figure biased toward angles higher than (counterclockwise to) the S axis, C1 will appear higher in contrast. Yet if the hue pair is instead rotated to angles below (clockwise to) the S axis, then stimulus C2 will appear more saturated, and the two should appear equal when the two angles are equidistant from the SvsLM axis. The mean angle of the pair at which the contrasts are judged to be equal thus defines the SvsLM axis. This angle was estimated by varying

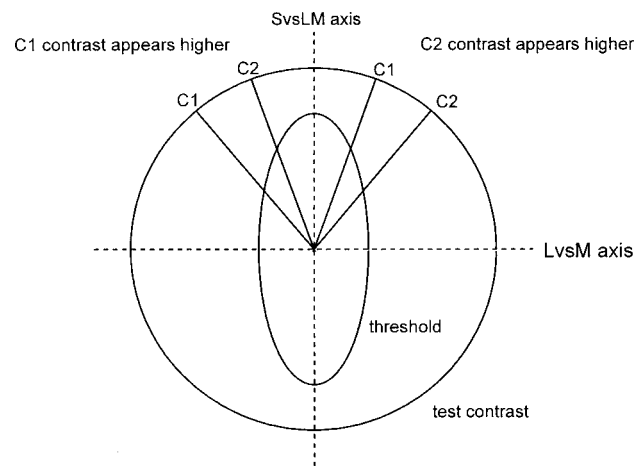


Fig. 2. Contrast matching task used to estimate the cone-opponent axes. Subjects were presented pairs of chromaticities (C1 and C2) that had the same contrast but differed by a fixed chromatic angle. The pair was rotated together around the color plane with staircases while subjects judged which of the two stimuli had the higher apparent contrast. Adaptation to a short-wavelength background selectively reduces sensitivity to the SvsLM axis, orienting threshold contours along this axis and reducing perceived contrast most for stimuli along the SvsLM axis. Thus the stimulus in the pair that is farthest from the SvsLM axis will appear to have the higher contrast, and the two should appear equal in contrast when the pair straddle the SvsLM axis equally.

the mean angle of the pair with four randomly interleaved staircases of ten reversals each. This method allowed observers to set the SvsLM and LvsM axes quickly and with good reliability. The resulting estimates are shown by the dashed lines in Fig. 1 and agree well with the axes estimated from the threshold contours.

3. Verification of the Cone-Opponent Axes

As noted, the LvsM and SvsLM axes that we measured deviated from the nominal cardinal axes. To confirm that the empirically defined axes were plausible, we tested for interactions between the axes, using a contrast adaptation task. Webster and Mollon^{8,25} showed that after the observer has adapted to a field that slowly flickers in color along the LvsM axis, all other axes appear rotated in hue away from the LvsM axis and toward the SvsLM axis. Thus if our estimates were correct, then adaptation to the empirical LvsM axis should not affect the perceived hue of stimuli confined to the empirical SvsLM axis. Alternatively, the perceived hue of stimuli along the nominal SvsLM axis should shift, toward the empirical axis. To test this possibility we used a hue-matching task, in which the observer (MW) compared the hue of physically identical stimuli presented to retinal areas under different states of adaptation. Stimuli were again presented in a pair of fields above or below fixation. The adapting stimulus was a 1-Hz sinusoidal modulation along MW's estimated L–M axis (-1.6 deg) and had a chromatic contrast of ± 60 . Adaptation was initially for 180 s and then for 6 s after each test presentation (see Webster and Mollon⁸). The test stimulus was a single chromaticity presented in both the top and bottom fields. The test contrast was fixed, while the hue angle defining the test was varied in two randomly interleaved staircases near

the +S (purple) or -S (yellow-green) axis. On each trial the observer judged whether the bottom field was “too red” or “too blue” (+S), or “too green” or “too yellow” (-S), compared with the color in the top field.

Figure 3 illustrates how the hue judgments should vary with the test angle. Adaptation to the LvsM axis selectively reduces sensitivity to the LvsM axis, thus collapsing the color space along this axis. When the test angle is clockwise from the +S axis, this will cause the perceived hue to become “more purple,” so that the bottom field will be rated “too red.” On the other hand, when the test angle is counterclockwise from the +S axis, then adaptation will rotate its apparent hue in the opposite direction (again toward the purple hue of the +S axis), so that the bottom, neutral adaptation field will instead appear “too blue.” Thus the stimuli should match in hue only when the hue angle lies along the S axis. (At this point

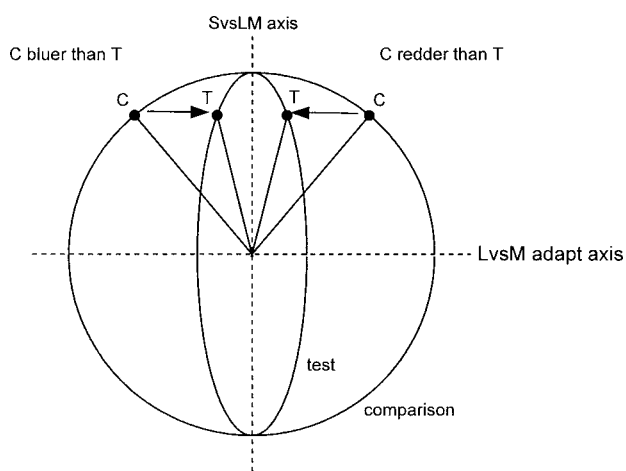


Fig. 3. Contrast adaptation task used to verify the cone-opponent axes. An asymmetric matching task was used to judge pairs of identical test stimuli under different states of adaptation. Adaptation to a modulation along the LvsM axis reduces perceived contrast along this axis and thus rotates perceived hue of test stimuli, T, toward the SvsLM axis. For hue angles clockwise from the +S axis, this causes the comparison stimulus (C, viewed under neutral adaptation) to appear redder than the test stimulus. For hue angles counterclockwise from the +S axis, the comparison stimulus instead appears bluer, and the test and comparison match in hue when they lie along the S axis.

the stimuli may still appear different in contrast, especially if the test contrast is low.⁸ To facilitate the judgments we therefore used a high test contrast of 60.)

The hue matches after adaptation to the empirical LvsM axis (-1.6 deg) had a mean value of 100.3 ($\sigma = 1.6$; $n = 8$) and 278.2 ($\sigma = 2.2$), very close to the estimated angle of the SvsLM axis (99.5–279.5 deg) but clearly different from the 90–270-deg nominal axis. (Note that the predicted match point for the nominal axes is slightly lower—at 88.4 deg—since the adaptation was to a nominal angle of -1.6 deg.) Thus the hue aftereffects agree well with the empirically defined axes. This is further illustrated in Fig. 4, which plots the psychometric functions for the hue judgments on the basis of the responses accumulated at each of the angles presented during the staircases. The two poles of the empirical SvsLM axis fall close to the midpoint of the functions, while stimuli along the nominal SvsLM axis were almost always rated as “too red” (+S) or “too green” (-S). These data thus suggest that the axes estimated on the adapting backgrounds do reflect the directions defining the LvsM and SvsLM axes.

4. Sources of Variations in the Cone-Opponent Axes

Figure 5 replots the estimates of the SvsLM and LvsM axes along with the range of angles predicted from known variations in peripheral color vision. Our analysis of these predicted variations is similar to the analysis reported by Smith and Pokorny.²⁶ In the present case we examined the range of variation suggested by individual differences in color matching. MacLeod and Webster²⁷ and Webster and MacLeod²⁸ used factor analysis to examine the sources of variability in the Stiles-Burch 10-deg color matching functions.²⁹ Among the factors identified were differences in lens density (estimated standard deviation across observers = 0.18 at 400 nm); macular pigment density ($\sigma = 0.18$ at 460 nm); the spectral peaks of the L ($\sigma = 50 \text{ cm}^{-1}$), M ($\sigma = 30 \text{ cm}^{-1}$), and S ($\sigma = 45 \text{ cm}^{-1}$) cones; and optical density of the photopigments ($\sigma = 0.045$). These factors were found to vary independently across observers. The horizontal lines at the top of Fig. 5 show the rotations in the LvsM or SvsLM axes predicted by a change of plus or minus two standard de-

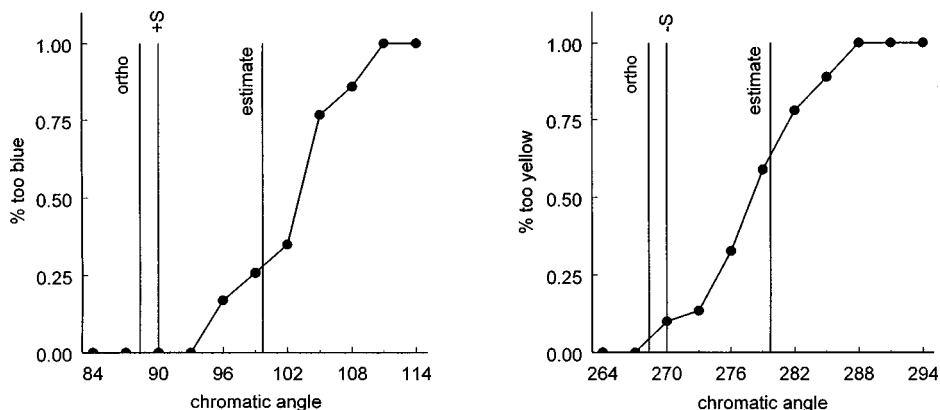


Fig. 4. Asymmetric hue matches following adaptation to the empirically defined LvsM axis (-1.6 deg, observer MW). Panels plot the psychometric functions for judging whether the comparison hue was too blue (left panel, +S axis) or too yellow (right panel, -S axis). For both poles of the SvsLM axis, hue matches occur at chromatic angles closer to the empirically defined SvsLM axis (99.5–279.5 deg) than to the nominal axis.

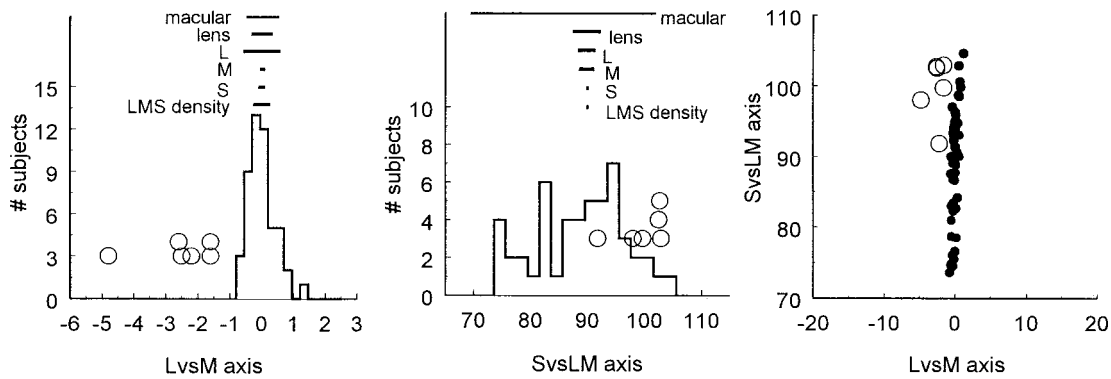


Fig. 5. Variations in the cone-opponent axes predicted by variations in peripheral color vision. Panels plot the range of angles predicted for the LvsM or SvsLM axes, on the basis of changes in the density of preretinal filters or in the spectral peaks or optical densities of the photopigments. Labeled bars give the range predicted by a variation of +2 standard deviations around the presumed mean value for each individual factor. Histograms plot the distribution of angles predicted by combining factors to reconstruct the spectral sensitivities presumed for 49 observers in the color matching data of Stiles and Burch (Ref. 29). Open circles plot individual axes estimated in the present study. Right panel compares the range of variation across the two axes, which for the simulated Stiles–Burch observers (filled circles) is ~ 15 times greater along the SvsLM axis when axes are scaled for equal multiples of threshold.

variations within each factor. These were estimated by adjusting the Smith–Pokorny³⁰ fundamentals for changes in each individual factor (following the assumptions for mean spectra described by Webster and MacLeod²⁸). The results illustrate how normal variations in these peripheral factors, and macular pigment variations in particular, can alter the cone-opponent axes of individual observers.²⁶

We also reconstructed the cone-opponent axes for the combinations of these factors predicted from individual observers' matches. In the analyses of MacLeod and Webster,^{27,28} an individual's value on each factor is given by the factor score (which expresses how many standard deviations the individual falls from the mean). These scores were used to define the fundamentals for each of the 49 observers, based on factors identified for lens and macular density and independent λ_{\max} shifts in the L, M, and S cones.^{27,28} These factors may not provide a strictly veridical account of the sources of the differences across observers (e.g., they may mask the modest differences predicted for photopigment density variations by absorbing the variance that is due to this factor²⁸), but they have the advantage that the fundamentals reconstructed from them are closely consistent with the differences in color matching among the Stiles–Burch observers. The distribution of axes predicted for these observers is shown by the histograms in Fig. 5 and spans a range of ~ 30 deg along the SvsLM axis and ~ 2 deg along the LvsM axis, given our scaling of the axes. (Within the original scaling of the MacLeod–Boynton diagram, the axes vary over a range of ~ 45 deg for the SvsLM axis and ~ 1.3 deg for the LvsM axis.)

By definition, the predicted distributions are centered on the angles of 90 and 0 deg defining the standard observer. In comparison, the axes measured in the present study are on average biased off these axes. Our estimates of the individual SvsLM axes fall within the range predicted for normal color variations (but are biased on average toward higher angles), yet the LvsM estimates lie outside this range. This difference is small (e.g., for a 30-times threshold stimulus the CIE 1931 x, y coordinates

are 0.325, 0.309 for the nominal +L axis and 0.326, 0.311 for the mean empirical axis at -2.6 deg). Nevertheless, the difference suggests that the parameters assumed for the standard observer and/or the stimulus calibration may have been in error, though we have not identified the source(s) of this discrepancy. [Varying a different set of standard fundamentals (e.g., those of Stockman *et al.*³¹) within a space defined by the Smith–Pokorny fundamentals produced only small changes in the mean angle of the cone-opponent axes. Similarly, introducing small errors into the estimated red phosphor spectrum, which is sharply peaked and thus most susceptible to measurement error, biased the mean chromaticity but added very little bias in the calculated directions, though we have not explored the effects of errors in combinations of phosphors.] In either case it is unlikely that the discrepancy results from an error in the assumptions underlying the empirical axis estimates, because these estimates agree with the angles implied by the adaptation-induced hue changes (see Fig. 4 and 7 below).

B. Sensitivity to the Cone-Opponent Axes

1. Thresholds

We used threshold contours on the neutral (30 cd/m², Illuminant C) adapting background to measure the relative sensitivity of the LvsM and SvsLM axes. In this case observers viewed the monitor directly, rather than through the beam splitter as in the measurements of Fig. 1. Ellipses were again used to approximate the contours and to define the sensitivity ratio. The mean thresholds along the LvsM and SvsLM axes remained close to pilot estimates on which we based the scaling of the axes. Thresholds along either axis varied over a roughly threefold range across the five observers, and the ratio of sensitivity to the two axes varied by roughly a twofold range (Table 1). We have not attempted to formally model the potential sources of this variation. However, differences in the relative sensitivity to the different axes could readily arise from a number of factors, including varia-

tions in the relative numbers of the three cone types, which show large individual differences.³²⁻³⁶

2. Contrast Adaptation

We also examined the relative sensitivity to the cone-opponent axes by examining changes in color appearance following color contrast adaptation. Scaling sensitivity on this alternative basis has the advantage that the test stimuli are suprathreshold and thus possibly more relevant to predicting suprathreshold vision, although it has the potential drawback that the scaling may be specific to

properties of the adaptation. As noted above, following adaptation to any color axis, the perceived hue of all other color directions is rotated away from the adapting axis and thus toward a second, null axis. For adapting angles intermediate to the cardinal axes, the angle between the adapting and null axes depends on the scaling of the color plane. For example, if the nominal scaling underestimates the SvsLM signals, then the measured nulls are biased toward the LvsM axis, or vice versa. The relative sensitivity to the cardinal axes in the adaptation task can thus be estimated by finding the relative scaling at which the adapting and the null directions are 90 deg apart (see Fig. 9 of Ref. 8). Webster and Mollon⁸ found that this scaling differed from the scaling predicted by their threshold estimates. We therefore attempted to use contrast adaptation to obtain a separate measure of the sensitivity ratio. A second goal was to use the hue changes to compare the scaling effects predicted by the nominal axis directions versus an individual observer's axes.

Subjects adapted in the field above fixation to a 1-Hz modulation of color along one of four chromatic angles in-

Table 1. S/LM Sensitivity Ratios Estimated from Detection Thresholds or Hue Shifts Following Adaptation

S/LM Ratio	JS	MW	VR	KL	GM	EM
Thresholds	1.75	1.04	0.94	0.8	0.75	—
Adaptation	—	1.72	1.13	1.31	1.17	1.00

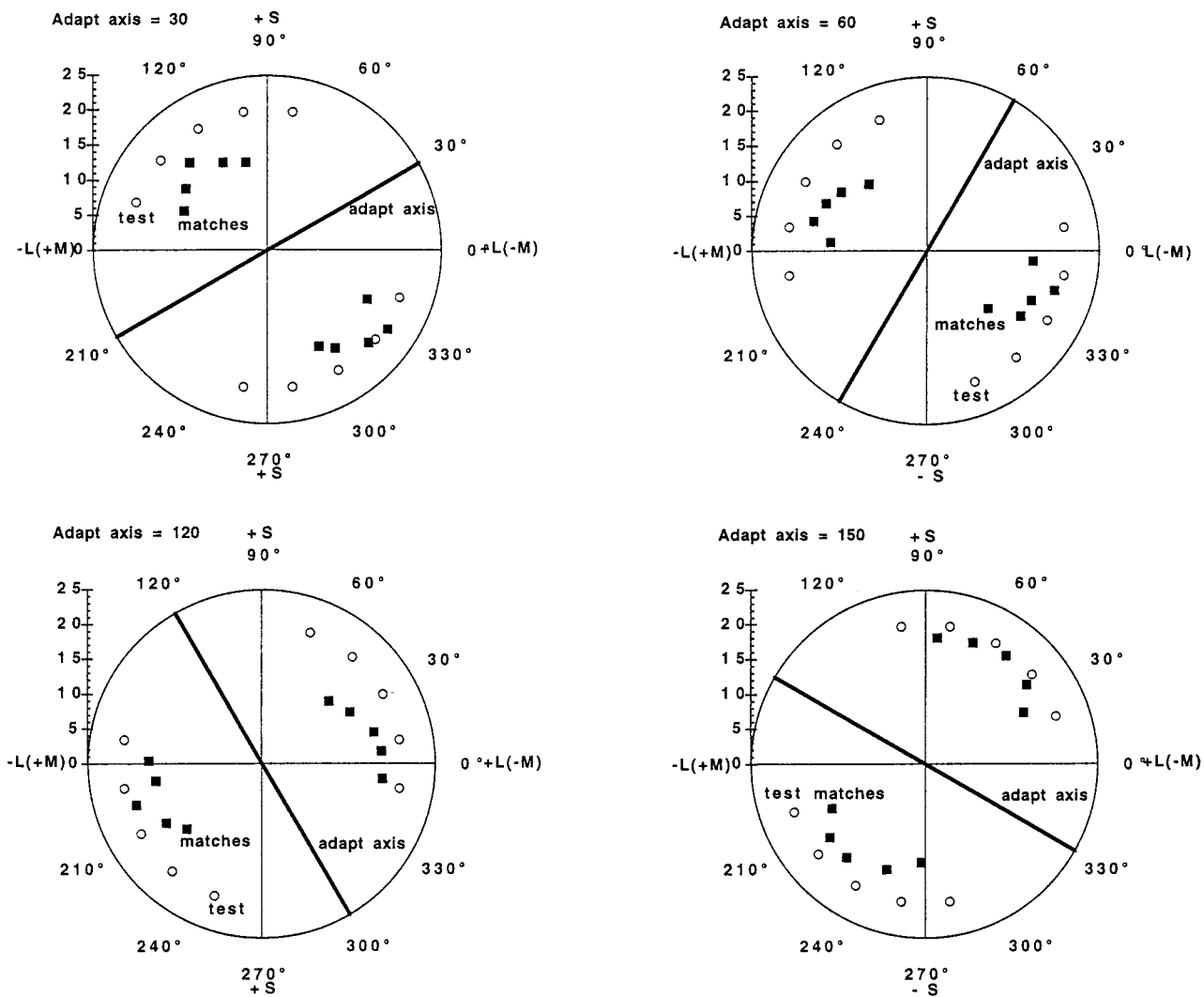


Fig. 6. Changes in color appearance following adaptation to different directions within the SvsLM and LvsM plane, for observer EM. Each panel plots the coordinates of test stimuli (open circles) and the matches made to them (filled squares) following adaptation to one of four adapting axes intermediate between the SvsLM and LvsM axes.

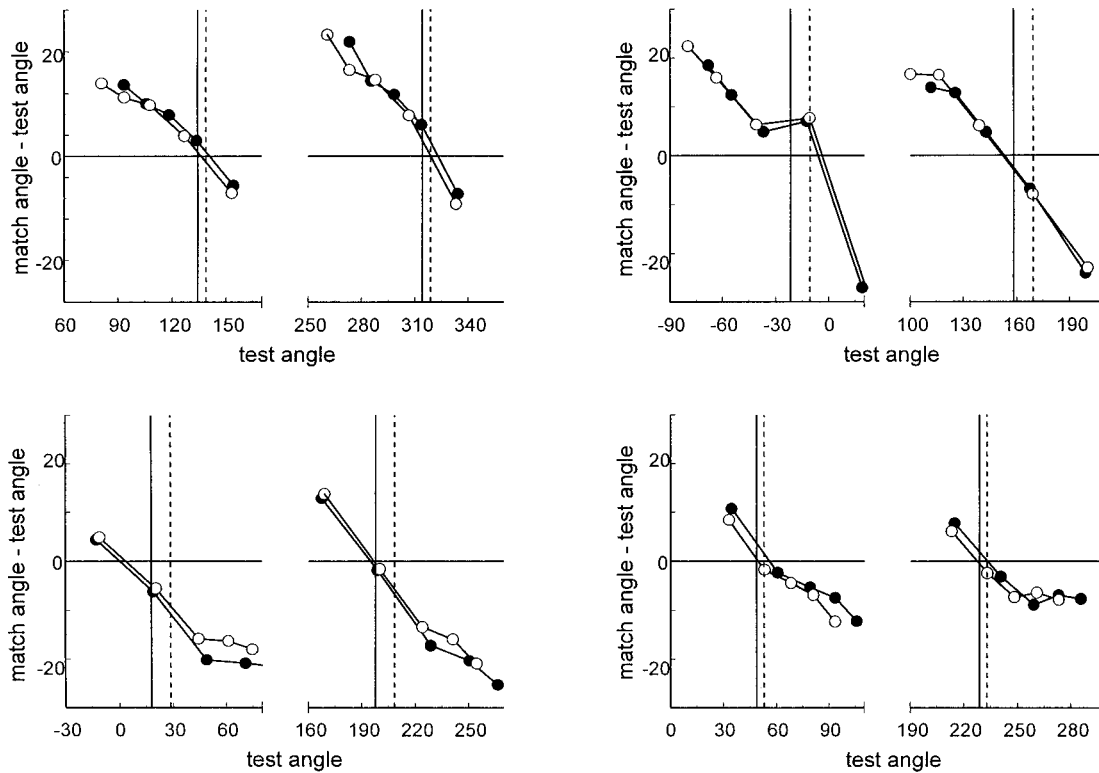


Fig. 7. Changes in the perceived hue of the test stimuli following adaptation for the matches shown in Fig. 6. Points plot the difference in angle between the test and the match. The four panels plot the results for the four different adapting axes for observer EM. For each, the pair of lines with filled symbols show the hue shifts following the best rescaling along the nominal cardinal axes, and the lines with open symbols plot the hue rotations within a space defined by the individual observer's SvsLM and LvsM axis directions. Vertical lines show the predicted angles at which tests should not appear rotated in hue, for the nominal axes (dashed lines) and for the individual observer's axes (solid lines).

intermediate to the LvsM and SvsLM axes. The adapting modulation varied over a range of ± 60 . A test color was then presented in the same field and was matched by adjusting the chromaticity in the matching field below fixation (following the same adapt and test sequence that we used in the measurements of Fig. 3). The tests differed in hue around a range of angles chosen to bracket the nominal null axis and had a fixed contrast of 20.

Figure 6 shows the color matches for one observer (EM). Each panel plots the test (open symbols) and matching (filled symbols) coordinates following adaptation to a different adapting direction. The matches reveal large and selective losses in sensitivity to each adapting axis, inducing rotations in the perceived hue angle of the test stimuli away from the adapting angle. Figure 7 shows the hue shifts more directly, by plotting the differences between the chromatic angles of each test and its selected match. The hue shifts in terms of the original axis directions, rescaled for the best-fitting sensitivity, are shown by the filled circles. If the nominal axis directions (0 and 90 deg) were appropriate for this observer, then it should be possible to scale relative sensitivity along these axes so that the hue shifts consistently change sign at test angles 90 deg from the adapting angle (as indicated by the dashed vertical line in each figure, which shows the predicted null direction for each adapting direction). Instead, the null axes deviate systematically from the nominal predictions. We therefore trans-

formed coordinates within the space by realigning the SvsLM and LvsM axes with the observer's estimated axes (102.5 and -2.5 deg) and then again varied the sensitivity ratio for the two axes to find the ratio that best normalized the nulls. Rotating the cardinal axes to correspond to the empirically defined axes reduced much of the error in the predicted nulls. This is shown by the open circles in Fig. 7, which plot the hue shifts within the individually defined space and which now change sign more consistently near the null axes predicted for this observer (solid vertical lines). For the four null axes, the rms deviation from the predicted 90-deg null was 4.3 deg, compared with 17 deg within the original, nominal color space. Improvements of similar magnitude were found for a second observer (MW). Like the results of Fig. 4, these suggest that our empirical estimates of the cone-opponent axes did identify the correct stimulus variations. However, for three further observers the residual errors were similar whether we assumed the nominal axes or their individual axes.

While rotating the axes improved the predictions for observer EM, rescaling the axes did not. That is, the best sensitivity ratio for predicting the nulls was found to be 1.0 and thus equal to the scaling based on mean thresholds. Alternatively, for four other observers the best fits were obtained after increasing the sensitivity assumed for the SvsLM axis (see Table 1). For these observers, the average S/LM ratio is 1.5 times greater for adaptation

than for thresholds, a value very similar to the difference assumed by Webster and Mollon.⁸ These results thus suggest that there may be modest but consistent differences between the sensitivities measured by the adaptation and by the thresholds. They also again point to individual differences in the relative scaling, which for the adaptation results varied over a roughly twofold range, similar to the range we observed in threshold-based estimates.

4. DISCUSSION

A. Variations in Cone-Opponent Axes

The LvsM and SvsLM cone-opponent axes have become increasingly popular as the stimulus dimensions chosen for probing postreceptoral color vision. Their widespread use stems from evidence that early stages of color coding are organized in terms of these dimensions.¹² Thus stimuli that vary along these axes may reflect more directly the characteristics of early postreceptoral color vision. However, to probe these axes implies that the chosen chromatic variations effectively modulate the signals along one of the axes while silencing the other, and few studies have sought to confirm this empirically. Our analyses reinforce the work of Smith and Pokorny²⁶ in showing that normal variations in human color vision must necessarily rotate the chromatic angles defining the cone-opponent axes for individual observers. Moreover, these axes are susceptible to calibration errors or stimulus inhomogeneities in the same way as are luminance variations—which are routinely characterized for individual subjects and testing conditions.¹⁴

We examined variations in the cone-opponent axes, using the chromatic adaptation procedure of Webster *et al.*²¹ and Webster and Mollon,⁸ and through this show significant biases in the SvsLM and LvsM axes for our observers. An advantage of this method is that the sensitivity changes are highly selective for chromatic angle and thus can provide a precise specification of the affected axes. A second advantage is that the two axes can be estimated independently by testing on long- or short-wavelength adapting backgrounds. Krauskopf *et al.*³⁷ suggested an alternative procedure for measuring the cone-opponent axes. When drifting vertical and horizontal gratings are superposed, they appear to move as a single coherent plaid when the component gratings are similar, while sliding independently past each other when the component gratings differ. Krauskopf *et al.* showed that the motion was least coherent when the two gratings varied along different cardinal axes. The LvsM and SvsLM axes could therefore be estimated by rotating the chromatic angles defining the gratings to define the point of minimal subjective coherence. By rotating grating pairs that differed by a fixed angle of 90 deg, they found a range of 30 deg in the estimated axes for three observers. However, since the two axes were yoked, this implies substantially larger rotations in the LvsM axis (up to 20 deg within their threshold-scaled space) than those that we observed or that would be predicted by normal variations in the cone spectra. (A problem inherent in estimating the two axes simultaneously is that for most choices of

scaling, the range of individual variation will differ substantially along the LvsM and SvsLM axes, and factors that affect the axes will thus more often lead to oblique—rather than orthogonal—rotations.) Further, because some sliding occurs between any pair of orthogonal angles within the chromatic plane, the coherence measure is not strongly selective for the specific color axes.

While there can be no question that the cone-opponent axes vary, it remains an important question whether and in what contexts these variations are large enough to influence observers' responses and thus whether they warrant specification for individual observers.²⁶ For luminance sensitivity it is well established that individual differences are critical to control for, and such controls are often considered a prerequisite for studies involving equiluminant stimuli. In these cases empirical estimates are important because observers are highly sensitive to the stimulus modulations introduced by errors in the presumed axes. For example, at higher spatial frequencies or for moving patterns, even a near-threshold luminance mismatch can strongly bias observers' judgments and thus bias the interpretation of results, and a major challenge under such conditions has been to develop methods that can reliably remove these potential artifacts.¹⁴ It is less clear to what extent similar problems arise with regard to errors along the two chromatic axes, for the spatiotemporal contrast sensitivity functions appear largely similar in shape along the LvsM and SvsLM axes, and their contributions to different tasks (e.g., to form or motion perception) appear similar. Smith and Pokorny²⁶ considered the effects of stimulus errors in threshold discrimination tasks and showed that these errors become pronounced only when the ratio of sensitivities along the different axes become large. Thus on neutral backgrounds, and with appropriate scaling of the axes, the errors associated with assuming the nominal observer may have little influence on measures such as discrimination ellipses. On the other hand, these errors could become pronounced when the scaling adopted leads to large sensitivity differences along the axes or when large sensitivity differences are induced by conditions that lead to differential adaptation. Indeed, it is the selective sensitivity changes with chromatic adaptation that underlies the technique that we used for defining the axes. Our results suggest that measurements under strongly biased states of chromatic adaptation should be highly sensitive to the choice of axes.

A second case in which our results point to the importance of empirical specification of the chromatic axes is in measurements that test for interactions between the axes. For example, we showed in Fig. 4 that following contrast adaptation to the LvsM axis, perceived hues shift toward the SvsLM axis. Yet this orthogonality is substantiated only for the empirically defined axes. When the same results are instead interpreted in terms of the nominal axes, then clear interactions are implied between the SvsLM and LvsM axes. Thus an error in the estimated axes could lead to different conclusions about the dimensions underlying color organization. Similar errors resulting from the nominal cardinal axes are also evident in the hue shifts shown in Fig. 7 and may be important in other tasks that depend on testing the

independence of the axes (e.g., as in the motion coherence paradigm of Krauskopf *et al.*³⁷).

ACKNOWLEDGMENTS

This research was supported by National Eye Institute grant EY-10834. We are grateful to David Brainard and John Werner for helpful comments on the manuscript.

Address correspondence to Michael A. Webster, Department of Psychology, University of Nevada, Reno, Reno, Nevada 89557; e-mail: mwebster@scs.unr.edu.

REFERENCES

1. R. L. De Valois, I. Abramov, and G. H. Jacobs, "Analysis of response patterns of LGN cells," *J. Opt. Soc. Am.* **56**, 966–977 (1966).
2. A. M. Derrington, J. Krauskopf, and P. Lennie, "Chromatic mechanisms in lateral geniculate nucleus of macaque," *J. Physiol.* **357**, 241–265 (1984).
3. J. Krauskopf, D. R. Williams, and D. W. Heeley, "Cardinal directions of color space," *Vision Res.* **22**, 1123–1131 (1982).
4. M. J. Sankeralli and K. T. Mullen, "Estimation of the L-, M-, and S-cone weights of the postreceptoral detection mechanisms," *J. Opt. Soc. Am. A* **13**, 906–915 (1996).
5. G. R. Cole, T. Hine, and W. McIlhagga, "Detection mechanisms in L-, M-, and S-cone contrast space," *J. Opt. Soc. Am. A* **10**, 38–51 (1993).
6. S. K. Shevell, "Redness from short-wavelength-sensitive cones does not induce greenness," *Vision Res.* **32**, 1551–1556 (1992).
7. C. F. Stromeyer III and J. Lee, "Adaptational effects of short wave cone signals on red–green chromatic detection," *Vision Res.* **28**, 931–940 (1988).
8. M. A. Webster and J. D. Mollon, "The influence of contrast adaptation on color appearance," *Vision Res.* **34**, 1993–2020 (1994).
9. J. D. Mollon, "'Tho' she kneel'd in that place where they grew ...,'" *J. Exp. Biol.* **146**, 21–38 (1989).
10. R. M. Boynton, A. L. Nagy, and C. X. Olson, "A flaw in equations for predicting chromatic differences," *Color Res. Appl.* **8**, 69–74 (1983).
11. C. F. Stromeyer III, A. Chaparro, C. Rodriguez, D. Chen, E. Hu, and R. E. Kronauer, "Short-wave cone signal in the red–green detection mechanism," *Vision Res.* **38**, 813–826 (1998).
12. M. A. Webster, "Human colour perception and its adaptation," *Network Comput. Neural Syst.* **7**, 587–634 (1996).
13. P. K. Kaiser, "Sensation luminance: a new name to distinguish CIE luminance from luminance dependent on an individual's spectral sensitivity," *Vision Res.* **28**, 455–456 (1988).
14. P. Lennie, J. Pokorny, and V. C. Smith, "Luminance," *J. Opt. Soc. Am. A* **10**, 1283–1293 (1993).
15. M. A. Webster, E. Miyahara, G. Malkoc, and V. E. Raker, "Variations in normal color vision. II. Unique hues," *J. Opt. Soc. Am. A* **17**, 1545–1555 (2000).
16. D. I. A. MacLeod and R. M. Boynton, "Chromaticity diagram showing cone excitation by stimuli of equal luminance," *J. Opt. Soc. Am.* **69**, 1183–1186 (1979).
17. D. H. Brainard, "Cone contrast and opponent modulation color spaces," in *Human Color Vision*, P. Kaiser and R. M. B. Boynton, eds. (Optical Society of America, Washington, D.C., 1996), pp. 563–579.
18. P. Cavanagh, D. I. A. MacLeod, and S. M. Anstis, "Equiluminance: spatial and temporal factors and the contribution of blue-sensitive cones," *J. Opt. Soc. Am. A* **4**, 1428–1438 (1987).
19. M. A. Webster and J. D. Mollon, "Colour constancy influenced by contrast adaptation," *Nature* **373**, 694–698 (1995).
20. M. A. Webster and J. D. Mollon, "Adaptation and the color statistics of natural images," *Vision Res.* **37**, 3283–3298 (1997).
21. M. A. Webster, K. K. De Valois, and E. Switkes, "Orientation and spatial-frequency discrimination for luminance and chromatic gratings," *J. Opt. Soc. Am. A* **7**, 1034–1049 (1990).
22. A. B. Watson and D. G. Pelli, "QUEST: a Bayesian adaptive psychometric method," *Percept. Psychophys.* **33**, 113–120 (1983).
23. M. A. Webster and J. D. Mollon, "Contrast adaptation dissociates different measures of luminous efficiency," *J. Opt. Soc. Am. A* **10**, 1332–1340 (1993).
24. E. Switkes and M. A. Crognale, "Comparison of color and luminance contrast: apples versus oranges?" *Vision Res.* **39**, 1823–1831 (1999).
25. M. A. Webster and J. D. Mollon, "Changes in colour appearance following post-receptoral adaptation," *Nature* **349**, 235–238 (1991).
26. V. C. Smith and J. Pokorny, "Chromatic discrimination axes, CRT phosphor spectra, and individual variation in color vision," *J. Opt. Soc. Am. A* **12**, 27–35 (1995).
27. D. I. A. MacLeod and M. A. Webster, "Factors influencing the color matches of normal observers," in *Colour Vision: Physiology and Psychophysics*, J. D. Mollon and L. T. Sharpe, eds. (Academic, London, 1983), pp. 81–92.
28. M. A. Webster and D. I. A. MacLeod, "Factors underlying individual differences in the color matches of normal observers," *J. Opt. Soc. Am. A* **5**, 1722–1735 (1988).
29. W. S. Stiles and J. Burch, "N.P.L. colour matching investigation: final report (1958)," *Opt. Acta* **6**, 1–26 (1959).
30. V. C. Smith and J. Pokorny, "Spectral sensitivity of the foveal cone photopigments between 400 and 500 nm," *Vision Res.* **15**, 161–171 (1975).
31. A. Stockman, D. I. A. MacLeod, and N. E. Johnson, "Spectral sensitivities of the human cones," *J. Opt. Soc. Am. A* **10**, 2491–2521 (1993).
32. C. M. Cicerone and J. L. Nerger, "The relative numbers of long-wavelength-sensitive to middle-wavelength-sensitive cones in the human fovea centralis," *Vision Res.* **29**, 115–128 (1989).
33. C. A. Curcio, K. R. J. Sloan, O. Packer, A. E. Hendrickson, and R. E. Kalina, "Distribution of cones in human and monkey retina: individual variability and radial asymmetry," *Science* **236**, 579–582 (1987).
34. C. A. Curcio, K. A. Allen, K. R. Sloan, C. L. Lerea, J. B. Hurley, I. B. Klock, and A. H. Milam, "Distribution and morphology of human cone photoreceptors stained with anti-blue opsin," *J. Comp. Neurol.* **312**, 610–624 (1991).
35. R. L. P. Vimal, J. Pokorny, V. C. Smith, and S. K. Shevell, "Foveal cone thresholds," *Vision Res.* **29**, 61–78 (1989).
36. M. F. Wesner, J. Pokorny, S. K. Shevell, and V. C. Smith, "Foveal cone detection statistics in color-normals and dichromats," *Vision Res.* **31**, 1021–1037 (1991).
37. J. Krauskopf, H.-J. Wu, and B. Farell, "Coherence, cardinal directions, and higher-order mechanisms," *Vision Res.* **36**, 1235–1245 (1996).